# Angular Scattering Analysis of the Circular Dichroism of Biological Cells. 2. The Red Blood Cell†

Adina Gitter-Amir,‡ Allan S. Schneider,¶ and Kurt Rosenheck*

ABSTRACT: A detailed interpretation of the grossly distorted ultraviolet absorption and circular dichroism spectra of the intact red blood cell is given, including an evaluation of the effects of protein conformation, detector geometry, cell hemoglobin content, and refractive index on the calculated cell spectra. The origins of the major differences between cell and hemoglobin solution spectra were quantitatively accounted for in terms of differential scatter and absorption flattening, with the latter effect dominating the picture. The relatively low sensitivity of the red blood cell suspension circular dichroism spectrum to hemoglobin conformation is due to the order of magnitude flattening of circular dichroism intensity. The importance of accounting for instrumental light detection geometry and the intense small angle scattering (<8°) for a range of particle sizes (0.1–5 μm) is made clear.

In the preceding paper we have calculated the corrected circular dichroism (CD)[1] spectrum for a suspension of red cell membranes (RCM) and determined their average protein secondary structure. We now use these results in a parallel analysis of intact human red blood cell (RBC) suspensions. We also consider partially hemolyzed red cells containing increasing amounts of hemoglobin (Hb) in order to illustrate the appearance of spectroscopic features characteristic of the large, absorbing, scattering particles, represented here by the RBC, and in general by most other biological cells. Our overall goal is to determine whether the highly distorted ultraviolet (uv) absorption and CD spectra of an intact biological cell can be quantitatively interpreted and the resulting corrected spectra used to derive conformational information about the cytoplasmic proteins within the cell.

The visible absorption spectra of RBC and of other biological particles have been analyzed by Latimer and co-workers (MacRae et al., 1961; Latimer and Eubanks, 1962; Latimer, 1967). Their initial corrections for scattering effects were based on a semiempirical treatment of scattering and on the theoretical relations derived by Duysens (1956) for the flattening effect. Later, the same authors used Mie scattering and anomalous diffraction calculations for the evaluation of visible spectra of a variety of particles including yeast cells, spinach chloroplasts, *Escherichia coli* cells, and RBC (Bryant et al., 1969; Latimer et al., 1968; Moore et al., 1968). Exact calculations of the dependence of extinction spectra of turbid suspensions of various biological particles on their volume and refractive index (Latimer and Pyle, 1972; Bryant and Latimer, 1969) and on photometer geometry were done by the same group (Latimer, 1975). Emphasis was laid on the special form of angular dependence of scattered light for large particles, where most of the scattered light is confined to a narrow cone in the forward direction. However, all these studies were confined to extinction spectra in the visible region, which contains information mainly about the heme chromophore and other nonpeptide chromophores of limited relevance to protein secondary structure.

Our extinction spectra studies are for the uv region of the spectrum and are extended to calculations of optical activity. Thereby we obtain information on the protein conformation of the cell contents. The uv region is also interesting for the possibility of estimating uv protein real refractive indices, which are difficult to determine experimentally. It should be remembered that the transition from the visible region (400–700 nm) to the uv protein absorption region (190–280 nm) involves a doubling in the size parameter of the particle (particle circumference/wavelength) and, therefore, the type of scattering phenomenon observed may be different.

The present analysis will have relevance to the spectroscopic properties of biological cells generally, as well as to other large (relative to wavelength) absorbing biological particles. In addition, there is the more specific interest in determining the structure of hemoglobin in situ within the red cell for a variety of pathological states of the erythrocyte, such as the sickle red blood cell. If we can derive this type of conformational information for the normal RBC, then it should be possible to perform a similar analysis with appropriate model scattering functions for the pathological red cell, and the various other hemoglobinopathies. This may be thought of as using molecular structure analysis to better understand some of the so called "molecular diseases". As can be seen in Figure 6 below (spectra marked Hb solution and RBC), there is an order of magnitude difference in $[\theta]$ between the experimental CD spectrum of intact red blood cells and that of hemoglobin in solution. There are several reasons for the gross difference in appearance between the spectra of a protein in solution and a protein inside a cell. In the calculational analysis presented below we attempt to clarify the sources of this difference. Specifically, we determine the sensitivity of the calculated turbid suspension spectra to (a) scattering acceptance angle and detector geometry, (b) trial input conformation, (c) he-

† From the Laboratory of Membranes and Bioregulation, The Weizmann Institute of Science, Rehovot, Israel A.G.-A., K.R.), and the Sloan-Kettering Institute for Cancer Research and Cornell University Graduate School of Medical Sciences, New York, New York 10021 (A.S.S.). *Received August 19, 1975.*

‡ This work derives in part from Adina Gitter-Amir's Ph.D. thesis (1974) carried out at the Feinberg Graduate School of the Weizmann Institute of Science, Rehovot, under the supervision of Dr. Kurt Rosenheck.

¶ Supported by National Institutes of Health Grants CA 08748 and CA 16889.

[1] Abbreviations used are: CD, circular dichroism; RCM, red cell membrane; RBC, red blood cell; Hb, hemoglobin; OD, optical density; Tris, 2-amino-2-hydroxymethyl-1,3-propanediol; NSF, number of significant figures.

moglobin content and optical density of the cell, and (d) cell cytoplasm refractive index. For particles the size of red blood cells, it is essential to consider the angular scattering contribution to CD and to absorbance for the particular instrumental detector geometries being used, since such large particles will have an intense small angle scattering contribution near the forward direction. Thus, a discrepancy can exist between a forward scattering calculation that counts scattering at all non-zero angles as excluded from the detector and an experimental measurement with a finite detector acceptance half angle, $\phi$ (8.5 ± 1.2° for Cary 6002 circular dichrometer), that excludes only scattering angles greater than $\phi$. Another reason for calculating the angular dependence of circular dichroism lies in the possibility that such angular optical activity may contain information on long-range order and supramolecular helical asymmetry, although we do not think this will be the case for the normal red blood cell.

Finally, we show the breakdown of the distortion in red cell spectra into differential scattering and absorption flattening contributions. The relative importance of the latter is made clear and should be considered when making measurements with instruments modified to remove only the differential scattering contributions.

## Experimental Methods

Human outdated blood, Rh positive, type O, was obtained from the blood bank of the Kaplan Hospital, Rehovot, and used in all our experiments.

Sphered RBC suspensions were prepared by suspending one volume of washed RBC in ten volumes of hypotonic phosphate or Tris-HCl buffer, pH 7.4. Various hypotonicities were tried, ranging from 130 to 200 mosM. For each osmolarity the RBC were checked in the phase microscope to see if sphering occurred, and centrifuged to see if a high Hb concentration was present in the supernatant, i.e., if hemolysis occurred. The highest tonicity buffer in which the RBC are sphered, with minimum hemolysis, was chosen as the buffer for the RBC suspension. This testing procedure is required for every blood sample, since different samples of blood begin to hemolyze in buffers of different osmolarity, probably because of the different average age of the RBC (and other unknown reasons). A small (<5%) amount of the older RBC will always have hemolyzed by this method. The resulting Hb and ghost fragments in the supernatant were washed out by repeated washes in the same buffer.

The concentration of Hb inside the cells in the final RBC suspensions was calculated from the total amount of Hb in the suspensions and the number of cells/cm$^3$. There was never more than 1% extracellular Hb present. The number of cells/cm$^3$ was determined from the volume of the pellet of a concentrated RBC suspension. The volume was determined by weight, using 1.1 g/cm$^3$ as the density and $\frac{4}{3}\pi r^3$, ($r$ = 3.26 $\mu$m) as the volume of the sphered RBC. The total Hb concentration was determined by hemolyzing a known volume of suspension in water, and measuring OD at 415 nm. $\epsilon_{Hb}$ at 415 nm was taken as 131 000 l.$^{-1}$ cm$^{-1}$ mol heme (U.V. Atlas of Organic Compounds). Optical density spectra were measured on a Cary 15 spectrophotometer. The half-acceptance angle, $\phi$, of the Cary 15, for a 1-mm cell is 8 ± 2° (see Gitter-Amir et al., 1976).

Circular dichroism measurements were made on a Cary 60 spectropolarimeter with a 6002 CD attachment in 1-mm cylindrical cells. The half-acceptance angle of this CD attachment is 8.5 ± 1.2°, for a 1-mm path length cell. Circular dichroism spectra were recorded in 20-nm stretches. After each stretch, the suspension was mixed and the last 10-nm stretch recorded again. A spectrum was considered acceptable if the repeated regions were superimposed. For OD spectra, after each spectrum the OD at the first wavelength was checked to correct for sedimentation effects. Measurements at short $\lambda$ ($\lambda$ < 210 nm) had to be made in phosphate buffers, because Tris buffer and chloride ion absorption is too high at the 150–200-mosM concentrations needed for RBC suspensions.

### *Calculation Methods*

The calculational scheme used is the same as the one described in part 1 (Gitter-Amir et al., 1976). Here, again, we use calculated extinction and CD spectra for $\phi$ = 8°, to compare with the experimental extinction spectra taken with 8 ± 2°, and experimental CD spectra taken with $\phi$ = 8.5 ± 1.2°. Because of the similar dependence of these spectra on half-acceptance angle $\phi$, all these angles give practically the same results. Calculated mean residue molar ellipticities representing scattering, absorptive, and total CD are denoted as $[\theta_S]$, $[\theta_A]$, and $[\theta_T]$, respectively. A comparison of the methods used in this analysis with the recent derivation of Bohren (1974, 1975a,b) was given in the preceding paper (Gitter-Amir et al., 1976).

### *Scattering Model*

The scattering model used for the sphered RBC and for the partially hemolyzed RBC is the coated sphere whose scattering functions are an extension of the Mie equations (Aden and Kerker 1951). The coat parameters are the best fitting parameters determined in Part 1 for the RCM. The core parameters are those of a Hb solution of the appropriate concentration. The Hb concentration in our sphered RBC is taken at 22 g/100 cm$^3$. It is smaller than the concentration in the biconcave disk RBC (34 g/100 cm$^3$) by the same factor as the volume increase on sphering (the volume increases from 94 to 145 $\mu$m$^3$). The experimentally determined values for the Hb concentration inside the sphered RBC were within 10% of this value. The Hb protein concentration relative to the membrane protein concentration, Hb/M, for the RBC is taken as 55. The concentration of Hb for partially hemolyzed RBC was adjusted according to the desired Hb/M ratio by partial hemolysis in a known volume of buffer.

The imaginary part of the refractive index of Hb, or $n_1'$, was determined from the absorbance. The molar absorbance for Hb was taken for several wavelengths from the U.V. Atlas of Organic Compounds (1966). For other wavelengths it was determined experimentally.

The real part of the refractive index in the visible, $n_1$, was adapted to our Hb concentrations inside the sphered RBC, from the calculated values of MacRae et al. (1961). For this purpose we used the following relation for protein solutions (Barer and Joseph, 1954)

$$n_{soln}(\lambda) = 1 + I(\lambda) \times C \qquad (1)$$

where $n_{soln}(\lambda)$ is the relative real refractive index of the solution, $I(\lambda)$ is the refractive index increment/concentration unit, and $C$ is the protein concentration in the same units. In the uv, neither experimental nor calculated values exist for the real refractive index of Hb solutions. The method described in Part 1 for estimating real refractive index values from comparison of calculated Mie extinctions with experimental extinction values is not practical for large, absorbing particles such as the RBC, for the following reasons. The forward ($\phi$ = 0°) extinction shows a periodic dependence on $n_1$, i.e., various values of $n_1$ correspond to the same forward extinction value (Figure

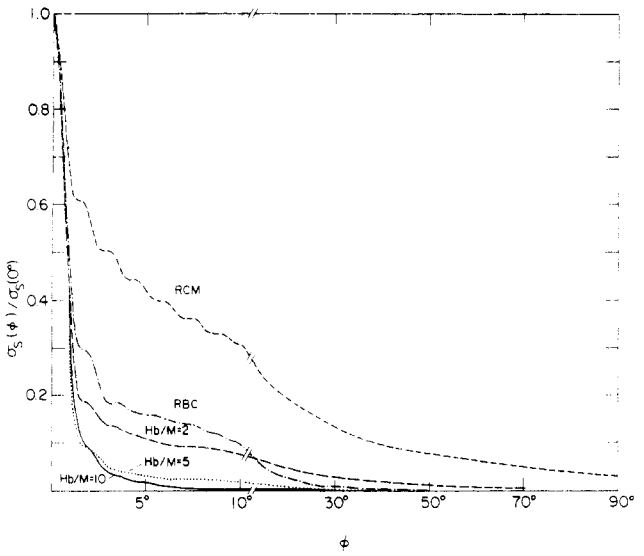


FIGURE 1: Dependence of the calculated relative scattering cross-section $\sigma_S(\phi)/\sigma_S(0)$ on the acceptance half-angle, $\phi$, for RCM, for sphered RBC, and for sphered partially hemolyzed red blood cells. λ 230 nm. (- - - - -) RCM, $m_2 = 1.14 - 0.0164i$; (- · - · -) RBC. $m_1 = 1.05 - 0.00017i$; (- - - -) partially hemolyzed RBC of Hb/M = 2, $m_1 = 1.001818 - 6 \times 10^{-6}i$; (· · · · ·) partially hemolyzed RBC of Hb/M = 5, $m_1 = 1.004545 - 16 \times 10^{-6}i$; (—) partially hemolyzed RBC of Hb/M = 10, $m_1 = 1.00909 - 30 \times 10^{-6}i$.

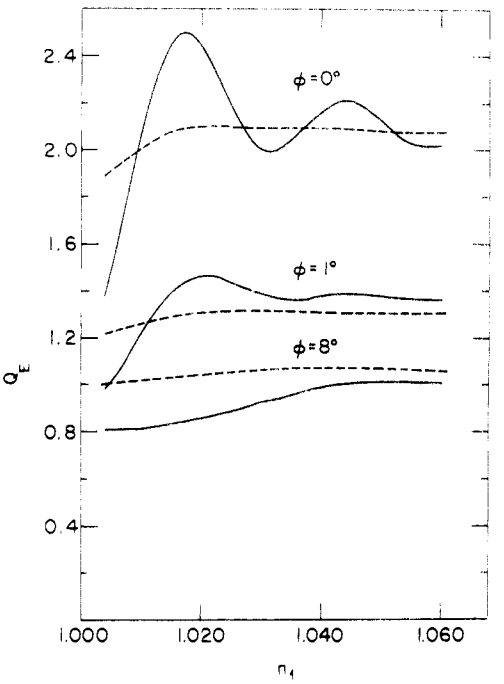


FIGURE 2: Dependence of the calculated total normalized extinction cross-section (efficiency), $Q_E$, of RBC on the real relative refractive index of the core, $n_1$, for various acceptance half-angles. (—) λ 230 nm, $n_1' = 0.00017$; (- - - - -) λ 210 nm, $n_1' = 0.00046$.

2, Results). This oscillation is damped when the absorption increases, which in turn causes the forward extinction at λ below ≃ 220 nm to be very insensitive to $n_1$ (Figure 2, Results). The extinctions calculated for $\phi > 1°$ are much smaller than the forward direction extinctions, since for RBC most of the scattered light is within a very narrow cone in the forward direction. Therefore, such calculations are again insensitive to $n_1$ (Figure 2, Results). For the same reasons, extinction calculations done for $\phi = 8°$, which corresponds to the measurement condition, are not very sensitive to the exact value of $n_1$. The calculated CD in the forward direction also shows a strong periodic dependence on the refractive index for $\lambda > 220$ nm. Therefore, if comparison of experimental and calculated data were to be done for $\phi = 0°$, a knowledge of $n_1$ would be required with an accuracy of ±0.02 for $n_1 < 1.04$ and ±0.05 for $n_1 > 1.04$, because of the nature of the $[\theta_S]_{0°}$ vs. $n_1$ curves. Since we use calculated $[\theta_S]_{8°}$ for comparison with experiment, the residual differential scattering is small, and the dependence on $n_1$ much smaller than for forward direction calculations. This, therefore, justifies our choice of one particular refractive index value. The value $n_{1,RBC} = 1.05$ corresponding to an $I$ value of 0.227 cm³/g was chosen. This value is in good agreement with values for Hb solutions extrapolated from the data of MacRae et al. (1961) and Orttung and Warner (1965). It also agrees with the values estimated for proteins by Holzwarth et al. (1974). We indicate, where required, the effects caused by changes in $n_1$ values. The $n_1$ values for partially hemolyzed RBC were calculated using $I = 0.227$ cm³/g.

The intrinsic protein optical activity for Hb was calculated from Chen et al. (1972), for 75% α helix and 0% β conformation. The solution optical activity spectra thus calculated were in very close agreement with experimental Hb solution spectra measured by Strauss et al. (1969). Optical activity data for Hb solution in the visible was taken from Urry and Pettegrew (1967).

The scattering functions, computer programs, and calculational checks are described in the Appendix.

## Results

In the results, which we present below, we first consider the sensitivity of the calculated spectra to the various parameters that enter both the calculation and the experimental measurement. In particular we have emphasized the effects of scattering acceptance half-angle, since this variable has a major effect on the calculated results, has not previously been calculated in this way for optical activity spectra, and has direct relevance to detector geometries of existing spectroscopic instrumentation. We calculate both absorption and circular dichroism spectra for sphered red blood cell suspensions, with the objective of (a) providing an interpretation of the gross differences observed between the spectra of the intact cell and the equivalent molecularly dispersed solution of the cell proteins, and (b) determining the precision with which reliable structural information can be derived from the CD spectra of an intact cell. Estimates of conformational sensitivity of calculated CD spectra will be useful for the latter purpose.

Figure 1 shows the effect of acceptance half-angle, $\phi$, on the relative scattering cross-section, $\sigma_S(\phi)/\sigma_S(0)$, for RCM, sphered RBC, and sphered partially hemolyzed cells containing varying amounts of hemoglobin. It can be seen that all the coated spheres considered have a much more intense small angle scattering than the RCM spherical shell. For all hemoglobin filled models, at a half acceptance angle, $\phi = 8°$, 90% of the scattered light is collected, and for an increased acceptance angle of $\phi = 90°$, more than 99% of the scattered light is being collected. However, for various coated spheres the dependence of $\sigma_S(\phi)/\sigma_S(0)$ is a function of both $\phi$ and $m_1$. It is the complicated periodic nature of the curves that makes it difficult to predict which of the models will have more intense small angle scattering and, thus, specific calculations for each set of parameters are required.

The nature of the Mie scattering characteristic of erythrocytes can be seen in Figure 2, where plots of normalized extinction cross-section (scattering + absorption) are shown as

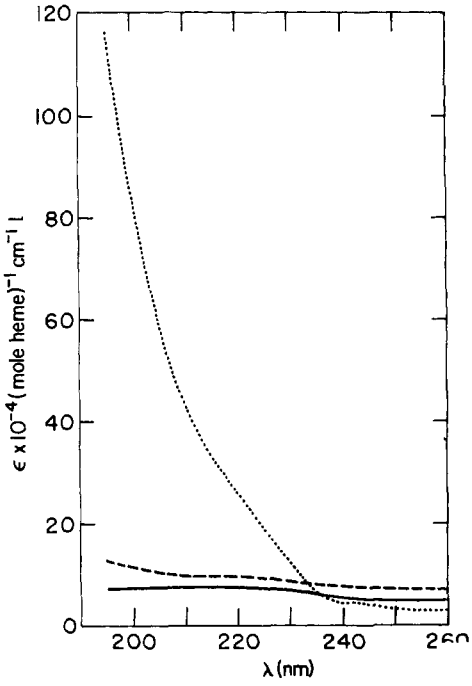


FIGURE 3: Calculated and experimental uv absorption spectra of RBC suspension and experimental spectra for Hb solution. (· · · ·) Hb solution spectrum; (- - -) RBC suspension spectrum, measured with $\phi = 8°$; (—) RBC suspension spectrum calculated for $n_1 = 1.05$, $\phi = 8°$.

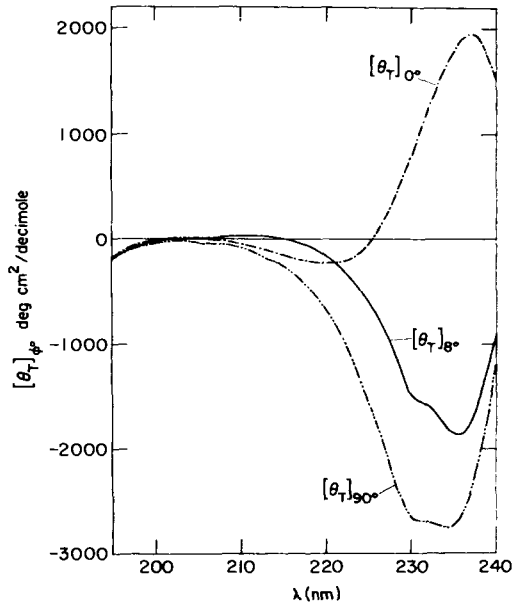


FIGURE 4: Dependence of calculated uv CD spectrum of RBC suspension on detector acceptance half-angle, $\phi$.

a function of real refractive index of the cell's interior, $n_1$. These plots are given for several detector acceptance half-angles, $\phi = 0°, 1°, 8°$, and for two wavelengths, $\lambda = 230, 210$ nm. At $\phi = 0°$ and $\lambda = 230$ nm, the characteristic Mie scattering oscillation of extinction cross-section with refractive index is seen. It is thus possible for such a case to have less scattering as the relative refractive index increases and the same type of behavior also exists with respect to cell size. At a wavelength of 210 nm, where absorption ($n_1'$) has increased considerably, the oscillations become damped out. Similarly, by going to larger acceptance angles, $\phi = 8°$, most of the scattered light is now collected by the phototube and again the oscillations, which are due to the scattered part of the total extinction, are removed and the extinction cross-section greatly reduced. Further properties of the Mie functions for large, absorbing, scattering particles can be found in standard scattering texts (van de Hulst 1957, Kerker, 1969).

Using the calculated values of extinction cross-section as a function of wavelength, it is possible to obtain a computed absorption spectrum for the red cell. In Figure 3 we compare such calculated spectra for $\phi = 8°$ with experimental spectra in the ultraviolet region. A contrasting experimental spectrum for a hemoglobin solution is shown in order to make apparent the extent of the distortion of the spectra for the intact cell. The cell suspension spectrum is seen to have a greatly reduced intensity near the uv absorption peak and to have a grossly flattened appearance relative to the solution spectrum. The fit of calculated and experimental spectra is quite good. A breakdown of the calculated spectra into absorption and scattering contributions indicates that the dominant effect in regions of absorption peaks is absorption flattening (Duysens, 1956), while in nonabsorbing regions the scattering dominates.

We now turn our attention to CD spectra for the red blood cell. The calculated effect of detector acceptance half-angle, $\phi$, on such spectra is shown in Figure 4. We consider angles, $\phi$, of 0°, 8°, and 90°. It can be seen that, while we would get a positive peak measuring in the strictly forward direction, we get a negative peak with $\phi = 8°$. The $\phi = 8°$ spectrum is more strongly influenced by pure absorption effects and is similar to the 90° spectrum, but the differential scattering effects cannot as yet be neglected. The spectrum calculated for $\phi = 90°$, is essentially the absorptive part of CD, and is indeed found to overlap the $[\theta_A]$ curve. It is interesting to note that $[\theta_T]_{90°}$, which thus represents an optical activity spectrum of RBC, corrected for scattering effects, is very much red shifted and distorted relative to a Hb solution spectrum (see Figure 6 below). The forward direction CD, $[\theta_T]_{0°}$ was calculated for $n_1 = 1.05$. The shape and magnitude of $[\theta_T]_{0°}$ are very strongly dependent on this parameter; for example, at $\lambda = 240$ nm, it is ca. $-2000$ deg. cm$^2$/dmol, for $n_1 = 1.04$ and for $n_1 = 1.06$, while for $n_1 = 1.05$ it is ca. $+1500$ deg. cm$^2$/dmol. The reason for the change in sign of $[\theta_T]_{0°}$ at $n_1 = 1.05$ is due to the change in sign of the slope of $Q_E$ vs. $n_1$ (Figure 2) compared to the slope at $n_1 = 1.04$. Schneider (1971) has previously noted the effects of the differential of extinction cross-section with respect to refractive index on the CD (eq. 15, in Schneider, 1971). The dependence of $[\theta_T]_{8°}$ on $n_1$ is an order of magnitude less sensitive, and, therefore, not so critical for comparison with our experimental spectra.

Figure 5 is the equivalent of Figure 4 for the visible region. Although the absolute magnitude of the peaks is smaller, we again see the importance of instrumental light detection geometry on CD spectra of cell size particles.

In Figure 6a we demonstrate the gradual appearance of the gross distortions in the uv CD spectra of the erythrocytes, by calculating spectra for red cells containing increasing amounts of Hb, up to the values present in the normal RBC. With increasing absorbance of the scattering particle, e.g., increasing hemoglobin content, the molar ellipticities become progressively diminished until finally, for the normal erythrocyte hemoglobin content (protein Hb/M = 55/1), the intensity of the CD bands has decreased more than an order of magnitude relative to the hemoglobin solution spectrum. In addition the normal 222-nm trough of the $\alpha$ helix of hemoglobin is considerably red shifted so that for the red cell it is at 235 nm. These are the dominant effects in the RBC spectra, and they

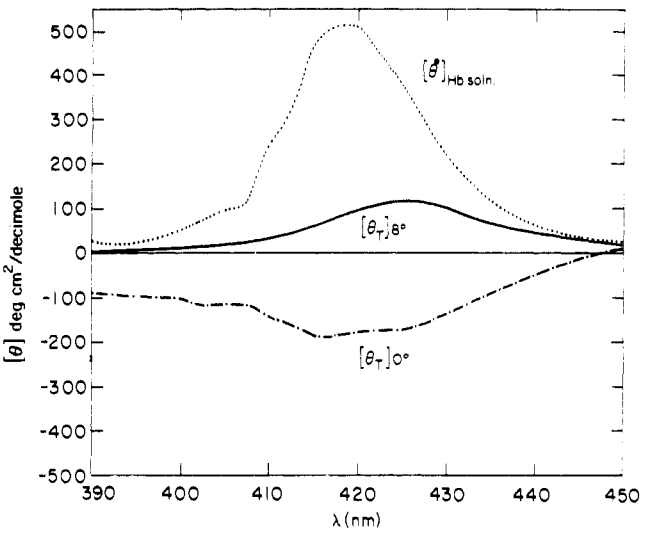


FIGURE 5: Dependence of calculated visible CD spectrum of RBC suspension on detector acceptance half-angle, $\phi$.

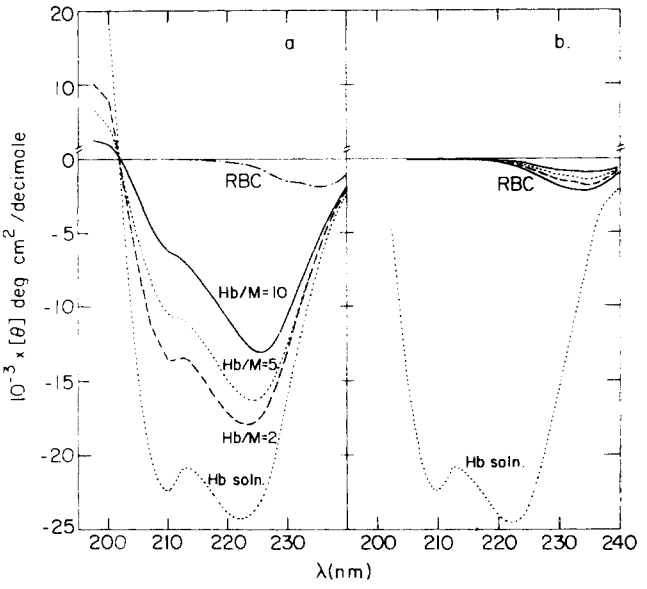


FIGURE 6: Dependence of calculated CD of RBC suspension on Hb properties: (a) sensitivity to Hb concentration in cell; the coat parameters are RCM parameters as used in part 1, Figure 5 (Gitter-Amir et al., 1976). The core is a Hb solution at the indicated concentration, with $m_1$ parameters as in Figure 1. (b) sensitivity to Hb conformation in cell: $n_1 = 1.05$. Upper (—) $\alpha = 30\%$, $\beta = 0\%$; upper (- - - -) $\alpha = 50\%$, $\beta = 0\%$; upper (– – –) $\alpha = 70\%$, $\beta = 0\%$; lower (—) $\alpha = 90\%$, $\beta = 0\%$; lower (- - - - -) Hb solution spectrum calculated for $\alpha = 75\%$, $\beta = 0\%$; rest unordered.

will influence our ability to extract protein secondary structures, as will be seen in the next figure.

Figure 6b provides a test of the conformational sensitivity of the calculated red blood cell CD spectra. Shown are turbid RBC suspension spectra calculated for several trial hemoglobin structures ranging from 30 to 90% $\alpha$ helix. Also shown is an input solution spectrum for the 75% $\alpha$ helix conformation in order to give perspective on the relatively small range of variation of calculated spectra for a wide set of trial structures. The same factors that dampen the total intensity of the RBC CD bands by an order of magnitude apparently also dampen the conformational sensitivity of the calculated suspension spectra. The result, unfortunately, is that the CD spectrum of the intact cell is considerably less sensitive to its protein conformation

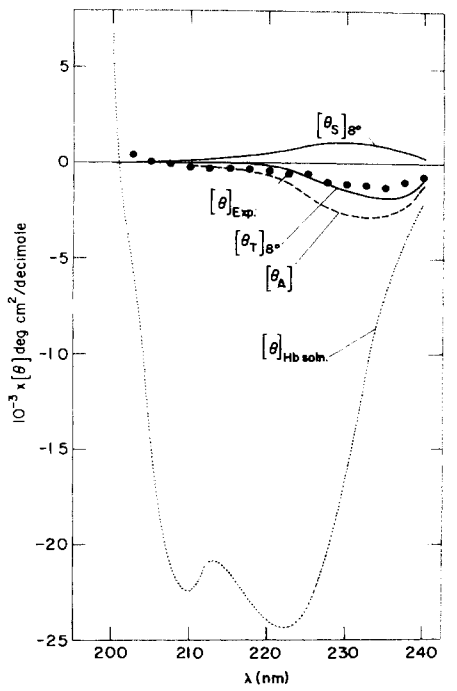


FIGURE 7: Comparison between experimental CD spectrum of RBC suspension and calculated $[\theta_T]_{8°}$. Also drawn are: $[\theta_S]_{8°}$, $[\theta_A]$, $[\theta]_{Hb\ soln}$.

than is, for example, either the spectrum of the membrane (Figure 4 preceding paper) or that of proteins in solution (Chen et al., 1972). In contrast to the RCM case where a 10% increment of $\alpha$ helix gave a molar ellipticity change of 2500 (deg cm²/dmol), for the RBC the same structural change results in a CD change of only about 300 (deg cm²/dmol).

If we take the calculated suspension CD spectrum ($\phi = 8°$) for a trial input structure of 75% $\alpha$ helix and no $\beta$ sheet, and compare it with an experimental sphered RBC spectrum we obtain the results shown in Figure 7. Again the hemoglobin solution spectrum is shown for perspective. The main point to be illustrated here is that the calculated RBC suspension spectrum agrees quite well with the experimental suspension spectrum, and, thus, accounts for the main distinguishing features of the circular dichroism of an intact cell. We can further determine the source of the gross differences between the spectrum of hemoglobin in solution and inside the red cell, by showing the breakdown of calculated suspension spectra into absorption and scattering contributions. The corresponding spectra are also shown in Figure 7 and it is readily apparent that the dominant effect on the red cell spectrum is absorption flattening (difference between $[\theta]_{Hb\ soln}$ and $[\theta_A]$) that accounts for the order of magnitude decrease in CD bands relative to the solution spectrum. The differential scattering contribution is seen to be small relative to the absorption flattening effect, although definitely there.

## Discussion

The ultraviolet CD and extinction spectra of turbid suspensions of RBC differ very markedly from the respective solution spectra of their components. This difference between the particle and the solution spectra is much larger than the differences that were found for spectra of membrane suspensions. In the latter, these differences could be classified as "distortions" and "shifts" but the main features of protein uv CD and extinction spectra were still recognizable. As we go from the RCM, to denser cells, e.g., partially hemolyzed RBC

of increasing Hb/M ratios, the effects caused by the absorbing nature of the particles become larger (Figure 6a). For an RBC suspension, the spectra look totally different from those of a Hb solution (Figures 3, 6, 7).

In the present work we have provided the first detailed interpretation of the ultraviolet absorption and circular dichroism of a simple biological cell. The sources of the major differences between cell and solution spectra were quantitatively accounted for in terms of absorption flattening and scattering contributions. The sensitivity of the calculated RBC spectra to protein conformation, detector geometry, refractive index, and hemoglobin content was determined and the role these variables play in defining the spectra of a cell was made clear. The relatively low sensitivity of the RBC suspension CD spectrum to hemoglobin conformation makes it difficult, though not impossible, to extract precise protein structural information, and this may be a general problem for large (>5 $\mu$m) highly absorbing cells. A much more exact knowledge of the other variables entering the calculation (e.g., complex refractive index, detector acceptance angle, cell size, and protein concentration) would be required if accurate protein conformations are to be obtained.

In the following, we shall discuss separately the contributions of differential absorption $[\theta_A]$, and of differential scattering $[\theta_S]_\phi$. It should be remembered, though, that the RBC suspension represents a case where $[\theta_A] + [\theta_S]_\phi \neq [\theta_T]_\phi$. The difference may be up to 10% since the particles are optically dense, and multiple forward scattering and absorption cannot be excluded (see Appendix).

The magnitude of $[\theta_A]$ and molar extinction coefficient, $\epsilon$, for the RBC suspensions are only ~10% of the respective solution values. This reduction is caused mainly by the "absorption flattening" effect (Duysens, 1956), which also causes the large red shift in the trough of the CD band. The trough of a Hb solution CD has an ellipticity of $[\theta] \simeq -24\,000$ deg cm$^2$/dmol, at 222.5 nm, while the trough of $[\theta_A]$ for the RBC suspension, at 235 nm has a value of $[\theta] \simeq -2500$ deg cm$^2$/dmol. The progressive flattening of the spectra was seen to occur with increasing hemoglobin content and absorption of the cell (Figure 6a).

The differential scattering contribution to the RBC CD spectrum is small relative to the magnitude of the solution spectra, but since $[\theta_A]$ is greatly reduced, the differential scattering contribution becomes of the same order of magnitude as the differential absorption contribution. This is in contrast to RCM and to partially hemolyzed RBC of low Hb/M, where $[\theta_S]_\phi$ is always much smaller than $[\theta_A]$. Therefore, in the case of a RBC suspension the differential scattering $[\theta_S]_\phi$ can influence the shape and magnitude of the CD spectrum.

The sign and the absolute value of $[\theta_S]$ are very strongly dependent both on $n_1$ and on $\phi$. We find that here, as in the case of the RCM, Mie scattering calculations for the forward direction are unsuitable for comparison with experimental spectra measured with half-acceptance angles larger than ~2°. For the forward direction, $[\theta_S]_\phi$ shows a large dependence on the relative real refractive indices, $n_1$. Therefore, for comparison with measurements made with $\phi = 0°$, one would have to know $n_1$ to an accuracy of $\pm 0.003$ for $\lambda \geq 220$ nm. (At lower wavelengths the magnitude of both $[\theta_S]_{0°}$ and $[\theta_A]$ is within the noise limits of the Cary 60 spectropolarimeter.) With $\phi \geq 1$-2°, the values of $[\theta_S]_\phi$ are much smaller than $[\theta_S]_{0°}$ values for $\lambda = 220$ nm (as mentioned above, at lower wavelengths, the absolute values of $[\theta_S]$ are very small, and it is difficult to establish an exact angular dependence). Since $[\theta_S]_{8°}$ is small, $[\theta_T]_{8°}$ represents a partly corrected spectrum, i.e., corrected for most of the differential scattering effects. This, in turn, implies a very small dependence of $[\theta_T]_{8°}$ on $n_1$. We do indeed find that our calculated $[\theta_T]_{8°}$ shows very close agreement with our experimental RBC suspension in CD, and that changing $n_1$ by $\pm 0.01$ units does not alter this agreement significantly.

The analysis of RBC suspension CD in terms of $[\theta_A]$ and $[\theta_S]_{8°}$ explains the low sensitivity of $[\theta_T]_{8°}$ to protein conformation within the cell. The main reason for this lack of conformational sensitivity is the fact that the cell spectra are reduced in intensity by an order of magnitude due to the absorption flattening effect. The result is that a change in protein conformation and trial intrinsic optical activity results in an order of magnitude, smaller change in RBC suspension CD, as was shown in Figure 6b. Thus, in order for these small changes in calculated CD spectra to distinguish accurately between various protein conformations, the noise level of the measured spectra must be very low and the accuracy and precision of the calculational input parameters must be quite high.

Several reports (Dorman et al., 1973; Philipson and Sauer, 1973; Gregory and Raps, 1974) have appeared in the literature, recently dealing with the experimental aspects of detector geometry on CD measurements, and these have been discussed in the preceding paper (Part 1). We wish to add a few comments here that came to light during the second part of this study on the intact RBC. First, it is important to note that for highly absorbing biological particles, a removal of the differential scatter by instrumentation having increased solid angle of detection does *not* result in a corrected CD spectrum ready for structural interpretation. This is because such a spectrum may still be grossly distorted by absorption flattening effects. For the red blood cell, these flattening effects dominate the spectral changes on going from hemoglobin in solution to hemoglobin within the cell and no matter how much of the differential scatter is experimentally collected, the resultant CD intensity will still be reduced an order of magnitude and have large distortions in shape and shifts in troughs. Secondly, it may be unnecessary to increase the acceptance angle beyond that of conventional instruments ($\phi \simeq 8°$) for many large biological particles, since most of the scattered light may have already been collected with the usual detection geometry. In Figure 8 we show the fraction of scattered light excluded by an 8° acceptance half-angle for various size particles with radii between 0.1 and 5 $\mu$m. Both the spherical shell and coated sphere models are shown, with complex refractive index of the shell being taken as that of our red cell membranes and the core being a 22% protein solution (hemoglobin). Particles with radii greater than 4000 Å are seen to have most of the scattered light collected by the conventional 8° acceptance angle (only 10% excluded for the coated sphere). Thirdly, for studies of differential scatter per se, a variation of acceptance half-angles from ~11 to 90° and greater as reported by Dorman et al. (1973) may miss most of the desired effect one is trying to see. Thus, if one wants to compare large and small solid angles of detection in order to observe the differential scatter for particles greater than 1 $\mu$m, the minimum possible acceptance angle consistent with instrumental noise ($\phi \leq 1°$) should be used for comparison with large angle detection geometry.

While the present work represents a prototype analysis of the uv absorption and circular dichroism of biological cells, we do not suggest or see any virtue in the random application of scattering analysis to cells or other biological particles that happen to have unusual spectra. Rather we suggest a case by

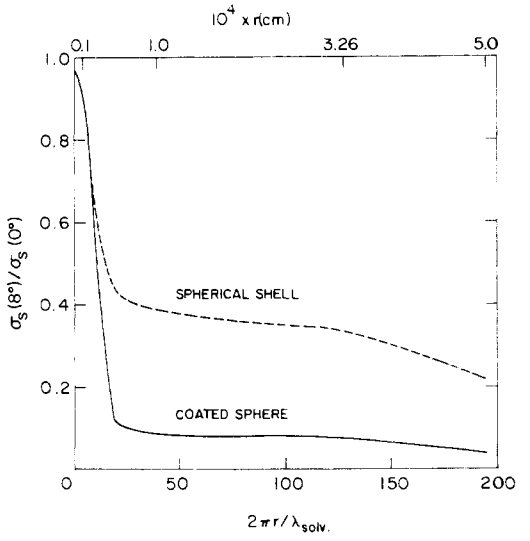


FIGURE 8: Dependence of the calculated relative scattering cross-section for $\phi = 8°$, $\sigma_S(8°)/\sigma_S(0°)$, on the size of the particle. $\lambda$ 225 nm; $r$: outer radius of the particle. (- - - -) Spherical shell particles with $\Delta = 10$ nm, $m_2 = 1.14\text{-}0.0162\,i$; (—) coated sphere particles with $m_1 = 1.05 - 0.0002 \cdot i$ and coat as above.

case consideration and application only to systems where relevant structural or other biological information is in the offing. Many examples of such systems can be cited of which the most immediate ones related to the present study would be the various pathological red blood cells and hemoglobinopathies such as sickle cell anemia and hereditary spherocytosis. Other interesting systems and applications include the in situ structure of nucleic acids in viruses and chromosomes, the spectroscopic identification and sorting of bacterial cells, and the interaction of various bioactive molecules, such as drugs and carcinogens, with cells. There is also the very interesting possibility that circularly polarized light scattering may contain information on long range order and supramolecular asymmetry of the scattering medium. It is obvious that the application of optical activity and polarized light scattering studies to complex biological structures is only in its infancy. We hope the present work contributes to its development.

Acknowledgments

We thank Miss A. Zakaria and Mrs. B. Romano for their skillful technical assistance and Mrs. Y. Sheraga for valuable assistance with the computer programming.

Appendix

Some important aspects of the Mie scattering computations of optical activity for suspensions of large absorbing particles were elaborated during this work. Since they are not mentioned in the literature on scattering of biological suspensions we shall summarize them here.

(*a*) *Separation of Scattering and Absorption Contributions to Suspension CD.* The separation of scattering and absorption contributions to suspension CD in the usual way (Schneider, 1973):

$$CD_T = CD_{scatt} + CD_{abs} \tag{1a}$$

is an approximation. It is true only for those cases where the extinction of a suspension of $N$ particles is $N$ times the extinction of a single particle, i.e., where Duysens' (1956) eq 2 may be linearly expanded. This is equivalent to saying that Beer's law holds for the suspensions (Duysens, 1956), which is also a criterion for single scattering (van de Hulst, 1957; Duysens, 1956). Systematic comparison of a large number of calculations with the linearly expanded and the logarithmic form of Duysens' equations for RBC at identical particle concentrations showed differences of 3–10% in $OD_{calcd}$ mainly at short wavelengths at which the extinction efficiencies have very large values. These results were obtained for particle concentrations and light paths as used in the experiments described. Thus, under these particular conditions the use of the linear expansion may lead to errors of the indicated magnitude, and for these cases we find indeed that $CD_T \neq CD_{scatt} + CD_{abs}$. It may be noted that the differences between the two types of calculation in the RCM case reach 1.5% at most and, thus, are negligible compared to the experimental errors.

(*b*) *Calculation of the Spherical Bessel Function of the First Kind, Half Integral Order $J_n(z)$.* Gordon (1972) mentions that $J_n(z)$ must be computed by backward recursion because the round-off error becomes too big otherwise. The recursion formula for $J_n(z)$ is:

$$J_{n+1}(z) + J_{n-1}(z) = (2n + 1/z)J_n(z) \tag{2a}$$

and the round-off error at each step:

$$\Delta J_{n+1}(z) = \Delta J_{n-1}(z) + (2n + 1/z)\Delta J_n + \Delta z \tag{3a}$$

If $(2n + 1) \sim |z|$ the round-off error will be the same whether the recursion is done backwards or forwards. Only when $2n + 1 \gg |z|$ must one use backward recursion. This was also pointed out by Espensheld et al. (1965).

(*c*) *Number of Significant Figures Needed at Different Stages of the Mie Scattering Computations.* The value of the complex argument $z = (x,y)$ of the Bessel functions determines the number of significant figures required in the computing procedure. For most values of $(x,y)$, $y$, the complex refractive index multiplied by the size parameter, is the determining factor. This can be shown as follows: using the notation of Pilat (1967) we have $Z_t^{(1)}(z)$: spherical Bessel function of the first kind and $Z_t^{(3)}(z)$: spherical Bessel function of the third kind, order $t$, where:

$$Z_0^{(1)}(z) = \frac{\sin z}{z};\ Z_1^{(1)} = \frac{\sin z}{z^2} - \frac{\cos z}{z} \tag{4a}$$

$$Z_0^{(3)}(z) = \frac{\sin z}{z} + \frac{\cos z}{z}$$

$$Z_1^{(3)}(z) = \frac{\sin z}{z^2} - \frac{\cos z}{z} + \frac{i\cos z}{z^2} + \frac{i\sin z}{z} \tag{5a}$$

Both $Z_t^{(1)}(z)$ and $Z_t^{(3)}(z)$ are calculated by forward recursion (Espensheld et al., 1965).

In the course of the Bessel function computations we have a small number that is calculated as the sum of numbers that can be very large. The number of significant figures needed (NSF) is:

$$NSF = OM|Z_0^{(3)}(z)| + OM|Z_0^{(1)}(z)| \tag{6a}$$

where OM is the order of magnitude.

It can be shown that

$$|Z_0^{(3)}(z)| < \frac{e^{|y|}}{|\sqrt{x^2 + y^2}|} \tag{7a}$$

and for most values of $(x,y)$

$$|Z_0^{(1)}| \sim \frac{e^{|y|}}{2\sqrt{x^2 + y^2}} \tag{8a}$$

For $(x,y) = (150,-15)$, which is the case for RCM at $\lambda \lesssim 200$ nm,

$$\mathrm{OM}|Z_0^{(3)}(z)| \sim 8 \text{ and } \mathrm{OM}|Z_0^{(1)}(z)| \sim 4 \qquad (9a)$$

and NSF is 12 for the calculation of the Bessel functions with one significant figure. Our calculated $Q_E$ value is a sum of Bessel functions and the calculated CD value is the small difference between $Q_E$ values. We thus find that at least 6 significant figures are required in the Bessel functions, in order to get 1 significant figure in the calculated CD value. Therefore, for $y$ values larger than 15, at least 19 significant figures are needed for the computation of CD values having 3–5 significant figures. In fact, in some of our calculations $y > 18$ because of the high $n_2'$ value at low wavelengths, and more than 30 significant figures are required. The Golem B computer of the Weizmann Institute of Science gives 19 significant figures in single precision and 38 significant figures in double precision. It was used in all cases when large $y$ values required more than 15 significant figures. All the other calculations were done on an IBM 370/165 computer in double precision (16 significant figures).

Our programs were checked against values for coated spheres with absorbing core (Fenn and Oser, 1965) and absorbing coat (Pilat, 1967), as well as nonabsorbing dielectric coated spheres (Kerker et al., 1962). Our angular scattering calculations were checked against values from Tables in Gumprecht and Sliepcevich (1953). Agreement was achieved in all cases.

## References


Aden, A. L., and Kerker, M. (1951), *J. Appl. Phys. 22,* 1242.

Barer, R., and Joseph, S. (1954), *Q. J. Microsc. Sci. 95,* 399.

Bohren, C. F. (1974), *Chem. Phys. Lett. 29,* 458.

Bohren, C. F. (1975a), Ph.D. Thesis, Department of Physics, University of Arizona.

Bohren, C. F., (1975b), *J. Chem. Phys. 62,* 1566.

Bryant, F. D., Latimer, P., and Seiber, B. A. (1969), *Arch. Biochem. Biophys. 135,* 109.

Bryant, F. D., Seiber, B. A., and Latimer, P. (1969), *Arch. Biochem. Biophys. 135,* 97.

Chen, Y. N., Yang, J. T., and Martinez, H. M. (1972), *Biochemistry 11,* 4120.

Dorman, B. P., Hearst, J. E., and Maestre, M. F. (1973), *Methods Enzymol. 27D,* 767.

Duysens, L. N. M. (1956), *Biochim. Biophys. Acta 19,* 1.

Espensheld, W. F., Willis, E., Matijevic, E., and Kerker, M. (1965), *J. Colloid Sci. 20,* 501.

Fenn, R. W., and Oser, H. (1965), *Appl. Opt. 4,* 1504.

Gitter-Amir, A., Rosenheck, K., Schneider, A. S. (1976), *Biochemistry 15* (preceding paper in this issue).

Gordon, D. J. (1972), *Biochemistry 11,* 413.

Gregory, R. P. F., and Raps, S. (1974), *Biochem. J. 142,* 193.

Gumprecht, R. O., and Sliepcevich, C. M. (1953), *J. Phys. Chem. 57,* 90.

Holzwarth, G., Gordon, D. J., McGinnes, J. E., Dorman, B. P., and Maestre, M. F. (1974), *Biochemistry 13,* 126.

Kerker, M., Kratohvil, J. P., and Matijevic, E. (1962), *J. Opt. Soc. Am. 52,* 557.

Kerker, M. (1969), The Scattering of Light and Other Electromagnetic Radiation, New York, N.Y., Academic Press.

Latimer, P. (1967), *Arch. Biochem. Biophys. 119,* 580.

Latimer, P. (1975), *J. Theoret. Biol. 51,* 1.

Latimer, P., and Eubanks, C. A. H. (1962), *Arch. Biochem. Biophys. 98,* 274.

Latimer, P., Moore, D. M., and Bryant, F. D. (1968), *J. Theor. Biol. 21,* 348.

Latimer, P., and Pyle, B. E. (1972), *Biophys. J. 12,* 764.

MacRae, R. A., McClure, J. A., and Latimer, P. (1961), *J. Opt. Soc. Am. 51,* 1366.

Moore, D. M., Bryant, F. D., and Latimer, P. (1968), *J. Opt. Soc. Am. 58,* 281.

Orttung, W. H., and Warner, J. (1965), *J. Phys. Chem. 69,* 3788.

Philipson, K. D., and Sauer, K. (1973), *Biochemistry 12,* 3454.

Pilat, M. I. (1967), *Appl. Opt. 6,* 1555.

Schneider, A. S. (1971), *Chem. Phys. Lett. 8,* 604.

Schneider, A. S. (1973), *Methods Enzymol. 27(D),* 751.

Strauss, J. H., Gordon, A. S., and Wallach, D. F. H. (1969), *Eur. J. Biochem. 11,* 201.

Urry, D. W., and Pettegrew, J. W. (1967), *J. Am. Chem. Soc. 89,* 5282.

U.V. Atlas of Organic Compounds (1966), Vol. 4, 54/2, DMS, London, Buttersworth.

van de Hulst, H. C. (1957), Light Scattering by Small Particles, New York, N.Y., Wiley.